ORGANOMETALLICS

Article

Cite This: Organometallics XXXX, XXX, XXX−XXX

Complexes of [(dadi)Ti(L/X)]^m That Reveal Redox Non-Innocence and a Stepwise Carbene Insertion into a Carbon−Carbon Bond

Spencer P. Heins,[†] Wesley D. Morris,[†] Thomas R. Cundari,[‡] Samantha N. MacMillan,[†] Emil B. Lobkovsky,[†] Nicholas M. Livezey,[†] and Peter T. Wolczanski*[,†]

[†]Department of Chemistry & Chemical Biology, Baker Laboratory, Cornell University, Ithaca, New York 14853, United States

[‡]Department of Chemistry, CASCaM, University of North Texas, Denton, Texas 76201, United States

Supporting Information

ABSTRACT: The addition of donors to (dadi)Ti(THF) (**1**-THF, dadi = [{−CH═N(1,2-C_6H_4)N(2,6-^{i}Pr$_2$−C_6H_3)}$_2$]^n) afforded the adducts [(dadi)Ti(L/X)]^m (**1**-L, m = 0, N_2CPh_2; m = −1, X = Cl$^-$, N_3^-, O^{i}Pr$^-$, CH_3^-, ^{neo}Pe$^-$, CH═CH_2^-, CCPh$^-$, CCTMS$^-$, H(D)$^-$). In all adducts, the chelate was in the (dadi)$^{4-}$ redox state. For certain anions, evidence for intimate binding of the Li$^+$ counterion was explored spectroscopically. Treatment of **1**-THF with $PhHCN_2$, yielded {PhC_3H_3(-NC_6H_4-2-NAr)$_2$}Ti(THF) (**3**, Ar = 2,6-^{i}Pr$_2$−C_6H_3), which contains a cyclopropanated dadi ligand. The mechanism was explored by calculations, and the addition of Ph_2CN_2 to **3** produced a nacnac derivative, {PhC(CHNC_6H_4-2-NAr)$_2$}Ti(η^2-HNNCPh_2) (**4**, Ar = 2,6-^{i}Pr$_2$−C_6H_3), generated via hydrogen transfer from the cyclopropane.

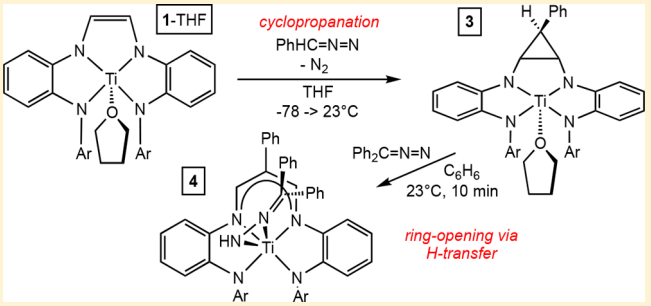

1. INTRODUCTION

In two recent communications, a diamide−diimine chelate, [{−CH═N(1,2-C_6H_4)N(2,6-^{i}Pr$_2$−C_6H_3)}$_2$]^n = (dadi)^n (n = 0 to −4)), was introduced as a designed redox noninnocent (RNI) ligand.[1,2] As illustrated in Scheme 1, complexes of iron and chromium, i.e., (dadi)M (M = Fe, Cr(THF)), reacted with organoazides[3−6] to afford nitrene-insertion products derived from aziridination followed by ring-opening, according to calculations.[1] Other products were generated from apparent nitrene insertion into C−H bonds when an electron deficient azide was the substrate. In both reaction sequences, products possessing higher formal oxidation states were not found to be particularly stable, according to calculations, and more oxidized redox states of the dadi ligand were not feasible. In fact, the reactivity could be rationalized by recognizing that iron did not vary from +2, and chromium was stable at a charge state between +2 and +3.[7]

According to calculations, electronic structures of the complexes, particularly (dadi)Cr(THF), proved to be intrinsically interesting. Metric parameters of (dadi)Fe were consistent with (dadi)$^{2-}$ chelating high spin (S = 2) Fe(II), i.e., {(dadi)$^{2-}$}Fe$^{\uparrow\uparrow\uparrow\uparrow}$, whereas the ground state of the chromium THF adduct was best described as an admixture of a (dadi)$^{3-}$ radical antiferromagnetically coupled to Cr(III) (S_T = 1), and an S = 1 excited state of (dadi)$^{2-}$ antiferromagnetically coupled to high spin Cr(II), i.e., α{(dadi)$^{2-}$}*$^{\downarrow\downarrow}$Cr$^{\uparrow\uparrow\uparrow\uparrow}$ + (1 − α){(dadi)$^{3-}$}$^{\downarrow}$Cr$^{\uparrow\uparrow\uparrow}$ with α > 0.5.

In the case of titanium, (dadi)Ti(THF) (**1**-THF) served as a source of (dadi)Ti (**1**) in the catalytic carbonylation of adamantyl azide to adamanyl isocyanate, AdNCO.[2] In this system, the electronic features of (dadi)^n are more readily seen, as (dadi)TiL$_x$ (**1**-L; x = 1, L = THF, PMe_2Ph; x = 2, L = CNMe) complexes are stabilized as Ti(IV) chelated by (dadi)$^{4-}$, whereas the metric parameters of (dadi)Ti═X (**2**═X; X = O, NAd) are consistent with (dadi)$^{2-}$. Although adduct-free (dadi)Ti (**1**) has not been isolated or spectroscopically observed, its calculated ground state (GS) is best ascribed as {(dadi)$^{3-}$}$^{\downarrow}$Ti$^{\uparrow}$, lending credence to descriptions of the effective charge on titanium as between +3 and +4.[7]

Herein further studies of [(dadi)Ti(L/X)]^m adducts and (dadi)Ti = X species are given in an attempt to further assay RNI character by spectroscopy and crystallography. In addition, attempts at generating alkylidene species[8] analogous to (dadi)Ti═NAd (**2**═NAd) have led to cyclopropanation chemistry, and calculations suggest that carbene transfer[9] from $PhHCN_2$[10] is more convoluted than the analogous nitrene transfer chemistry.

2. RESULTS

2.1. Adducts of (dadi)Ti (1). *2.1.1. [(dadi)Ti(L/X)]^m (L = ClLi(THF)$_4$, 1-Cl·Li; THF, 1-THF).* Initial attempts at the synthesis of (dadi)Ti (**1**) were conducted via metathesis as Scheme 2 describes. After generating green (dadi)Li_2 *in situ*, the addition of (tmeda)$_2$$TiCl_2$[11] afforded a dark green solution

Special Issue: In Honor of the Career of Ernesto Carmona

Received: April 5, 2018

DOI: 10.1021/acs.organomet.8b00188
Organometallics XXXX, XXX, XXX−XXX

Scheme 1. Previous Studies Revealed Nitrene Insertions, Likely via Aziridine Transients, and the Catalytic Carbonylation of AdN_3 by (dadi)Ti (1), a Process That Utilizes the Redox Non-Innocence (RNI) of (dadi)^n

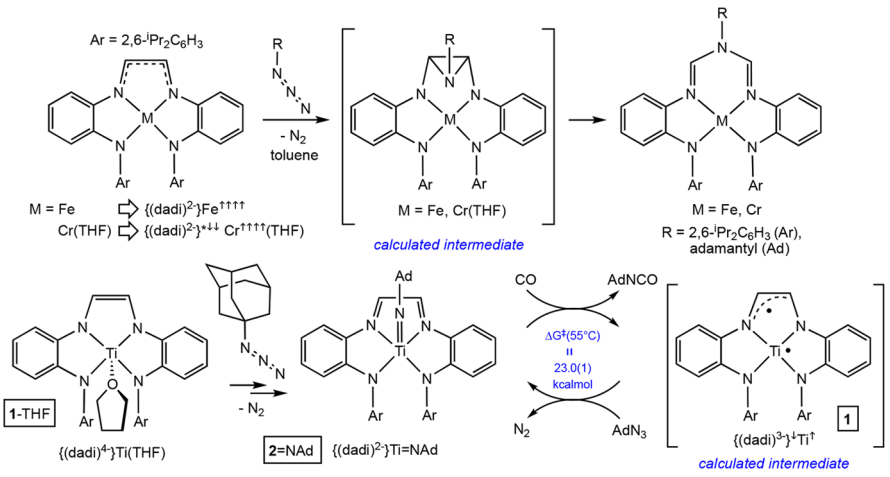

Scheme 2. Metatheses of $(tmeda)_2TiCl_2$ with $(dadi)M_2$ Afford Different Adducts Depending on M

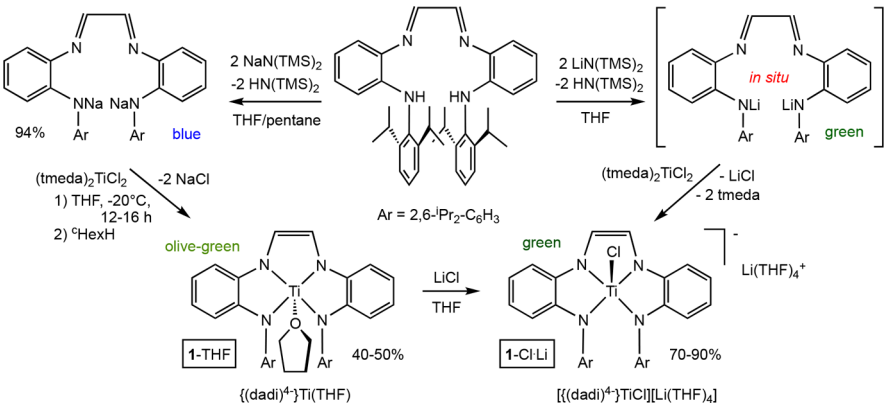

from which the chloride adduct, [(dadi)TiCl][Li(THF)$_4$] (**1**-Cl·Li) was isolated in ∼90% yield. Attempts to displace Cl^- from **1**-Cl·Li proved difficult, hence it was reasoned that the significantly less soluble NaCl should be targeted as a biproduct. The switch to (dadi)Na_2, which was isolated as a blue solid in 94% yield,[2] afforded the olive-green THF adduct, (dadi)Ti(THF) (**1**-THF),[2] in 40−50%. Fortunately, **1**-THF was found to be a much more labile starting material and was used almost exclusively in the remaining synthetic studies.

2.1.2. General Synthesis of [(dadi)Ti(L/X)]^m. Preparation of the THF complex, (dadi)Ti(THF) (**1**-THF), afforded a ready means of preparing a variety of adducts via simple substitution. Scheme 3 portrays the adducts, which were synthesized in THF in roughly 40−90% yields as given. Each adduct was determined to be five-coordinate, by virtue of observing four independent isopropyl Me groups in ^{1}H NMR spectra. As previously noted, the 2,6-^{i}Pr$_2$−C$_6$H$_3$ aryl groups are aligned roughly face-to-face in the dadi ligand, and rotation about the *ipso*-carbon−nitrogen bonds are severely hampered by sterics upon chelation to a metal. Consequently, the isopropyl Me groups are diastereotopic and are observed as two doublets if two mirror planes are present, and four doublets if one mirror plane is present, as in the case of the 5-coordinate adducts, although they are often overlapping. In related ligand systems, it is often possible to distinguish between the two redox forms of the ligand through routine chemical shift changes in ^{1}H NMR spectra.[12,13] In the case of $(dadi)^{2-}$, the sp^2 backbone imine protons are of interest, but in the reduced $(dadi)^{4-}$ form of the ligand, the same protons are also sp^2 by virtue of being attached to the olefin. Experimentally, there is no significant difference between the shifts of the dianion and the formal tetraanion, hence distinguishing between ligand redox states necessitates structural information.

The addition of sodium azide to form [(dadi)TiN_3][Na(15-c-5) (**1**-N_3·Na) was conducted in the hope of generating $[\{(dadi)^{2-}\}Ti^{IV}N]^-$, but a variety of thermal and photochemical attempts were unsuccessful at cleanly forming the nitride anion.[14−23] The IR spectrum of **1**-N_3·Na manifested a $\nu(N_3)$ at 2077 cm^{-1}, consistent with a simple azide complex. Similarly, treatment of (dadi)Ti(THF) (**1**-THF) with $Ph_2C{=}N{=}N$ failed to elicit the generation of N_2 and the diphenylalkylidene complex.[24−33] Instead, a simple green adduct,[34] (dadi)Ti(N=N=CPh_2) (**1**-NNCPh_2), was observed, and calculations (*vide infra*) suggest it is η^2-N_2CPh_2. The bronze-colored isopropoxide derivative, [(dadi)Ti(O^{i}Pr)][Li(THF)$_4$] (**1**-O^{i}Pr·Li), is tentatively formulated as an ion pair due to the observation of THF molecules that persist in benzene-d_6 solution.

2.1.3. Selected NMR Spectroscopic Features of [(dadi)Ti(L/X)]^m. As the X-ray crystal structures (*vide infra*) and some NMR spectra indicate, structural ambiguities persist in whether the main group counterion is an integral part of the complex

DOI: 10.1021/acs.organomet.8b00188
Organometallics XXXX, XXX, XXX−XXX

Scheme 3. Various Adducts Prepared from (dadi)Ti(THF) (1-THF) and Suitable Reagents in THF[a]

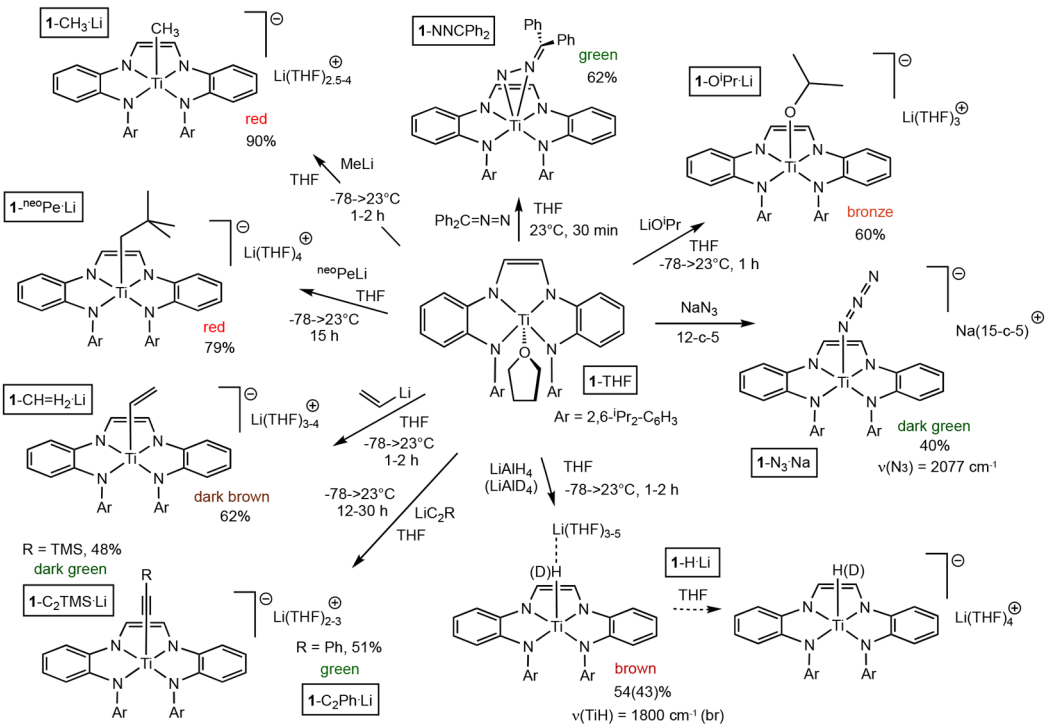

[a]Precipitation or crystallization was from pentane in most cases.

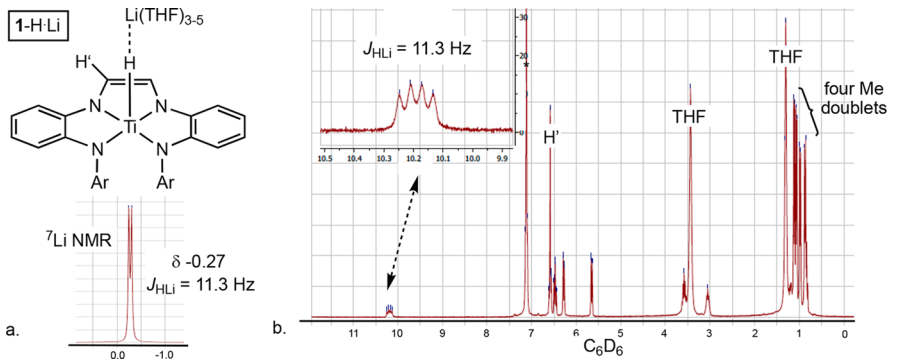

Figure 1. NMR spectra of the hydride anion, $[(dadi)TiH][Li(THF)_3]$ (**1**-H·Li) in C_6D_6: (a) ^{7}Li NMR spectrum showing J_{HLi}. (b) ^{1}H NMR spectrum showing J_{HLi}, the diamide methine, the four methyl doublets that indicate 5-coordination, and the remaining resonances attributable to aryl and Me_2CH groups.

via binding to X^- or through complexation to the $C_2N_2^{2-}$ part of the dadi^{4-} backbone. Hydrocarbyl adducts manifest shifted ^{1}H and ^{13}C{^{1}H} resonances upon complexation in addition to color changes from the green hue of (dadi)Ti(THF) (**1**-THF) to a typical red/red-brown coloration of the adducts. The Ti–CH_3 unit of (dadi)Ti(CH_3)·Li$(THF)_2$ (**1**-CH_3·Li) was observed as singlets at δ 0.79 in the ^{1}H NMR spectrum, and δ 36.07 in the ^{13}C{^{1}H} NMR spectrum. Curiously, the ^{1}H NMR spectral shifts for the ^{neo}Pe group in (dadi)Ti(^{neo}Pe)·$Li(THF)_{2.4}$ (**1**-^{neo}Pe·Li) appear in a "normal" range at δ 1.21 (CH_2) and δ 0.89 (Me_3), but the corresponding ^{13}C resonances are shifted considerably: $TiCH_2$, δ 86.83; C_β, δ 39.94; $(CH_3)_3$, δ 34.8.

The vinyl derivative, (dadi)Ti(CH═CH_2)·$Li(THF)_{3-4}$ (**1**-CH═CH_2·Li) manifests a non-first-order ABX pattern in its ^{1}H NMR spectrum, necessitating a simulation: δ 8.2265, $C_\alpha H$, J_{trans} = 20.90 Hz; J_{cis} = 14.65 Hz; δ 6.0046, $C_\beta HH$, J_{trans} = 20.90 Hz, J_{gem} = −4.20 Hz; $C_\beta HH$ at δ 5.9995, J_{cis} = 14.65 Hz, J_{gem} = −4.20 Hz. While lithium–carbon coupling (^{7}Li (I = 3/2, 92.5–96%))[35] does not appear in this sp^2-hydrocarbyl derivative, the ^{13}C{^{1}H} NMR spectrum of [(dadi)TiCCPh]-$[Li(THF)_2]$ (**1**-CCPh·Li) exhibited a quartet at δ 138.72 with a J_{CLi} of 6.8 Hz, suggestive of a significant C_α–Li interaction in benzene-d_6 solution. No coupling was observed for C_β (δ 142.69), nor was any lithium–carbon coupling observed in the corresponding trimethylsilylacetylide derivative, [(dadi)-$TiCCSiMe_3][Li(THF)_2]$ (**1**-CCTMS·Li), whose C_α-shift at δ 162.27 was at considerably lower field than the phenylacetylide derivative. The remaining resonances in both alkynyl anions are quite similar.

2.1.4. Spectroscopic and Dynamic Features of (dadi)TiHLi (1-H·Li). The hydride anion, $[(dadi)TiH][Li(THF)_2]$ (**1**-H·Li), features a quartet at δ 10.22 (J_{HLi} = 11.3 Hz)[35] in its ^{1}H NMR spectrum in C_6D_6, as Figure 1 illustrates. To distinguish

DOI: 10.1021/acs.organomet.8b00188
Organometallics XXXX, XXX, XXX–XXX

Table 1. Diffusion Coefficients for Individual dadi, THF, and Lithium Resonances as Determined by ^{1}H and ^{7}Li DOSY Experiments[a,b]

^{1}H (δ) C_6D_6	D (cm^2/s) ($\times 10^6$)	^{1}H (δ) THF-d_8	D (cm^2/s) ($\times 10^6$)	^{7}Li (δ)	D (cm^2/s) ($\times 10^6$)
0.9	4.13(3)	0.84	5.00(3)	−0.27 (C_6D_6)	5.2(1)
1.01	4.04(3)	3.21	5.2(1)	−0.49 (THF-d_8)	5.5(4)
1.09	4.11(3)	5.18	4.9(2)		
1.14	4.10(3)	6.05	5.0(2)		
1.32[c]	8.9(9) 67%	6.18	4.9(2)		
	4.6(9) 33%	6.24	4.9(2)		
3.08	4.0(1)	6.44	4.9(2)		
3.45[c]	8.7(6) 73%	6.89	4.85(4)		
	4.5(9) 27%	10.46	4.9(3)		
3.61	4.5(1)				
5.68	4.1(1)				
6.31	4.10(6)				
6.5	4.1(1)				
6.63	4.10(3)				
10.22	4.1(2)				
avg	4.1(2)[d]		5.0(5)		

[a]Diffusion coefficients were measured using double pulsed gradient stimulated spin−echo (DPGSE) experiments with convection compensation using the DgscsteSL_cc or Dbppste_cc pulse sequence as provided in VnmrJ 3.2 at 295 K. The ^{7}Li signal in C_6D_6 was ^{1}H-decoupled. The following parameter values were used: ^{1}H nucleus, δ = 0.0018 s, Δ = 0.1244 s; ^{7}Li nucleus, δ = 0.004 s, Δ = 0.0987 s. Gradient strength was varied from 2.1 to 58.6 G/cm in 24 linear increments. [b]D was determined from plots of $\ln(I/I_0)$, the integrated intensities, vs $\delta^2\gamma^2(\Delta-\delta/3)G^2$, where the constants have their usual definitions; see the Supporting Information for the relevant equations and details. Igor Pro was used for the fits and the reported errors. [c]Deviation from linear behavior was observed, indicating free and bound THF in C_6D_6 prompting biexponential decay fits. [d]THF (biexponentially determined D's) not included.

Table 2. Comparative Distances (Å) of {(dadi)$^{4-}$}TiL$_x$ (1-L$_x$) and {(dadi)$^{2-}$}Ti═X (2═X)[a]

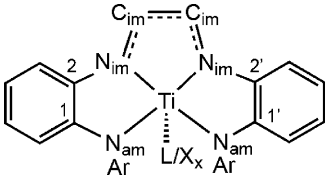

compd	TiN$_{im}$	TiN$_{am}$	C$_{im}$C$_{im}$	C$_{im}$N$_{im}$	C^{1}N$_{am}$	C^{1}C^2	C^{2}N$_{im}$	TiL/X
1-Cl·Li	1.999(4)	2.008(4)	1.343(7)	1.371(6)	1.402(6)	1.411(6)	1.391(6)	2.310(2)
	2.044(4)	2.018(4)		1.382(6)	1.422(5)	1.413(6)	1.392(6)	
1-CH$_3$·Li[b]	2.021(2)	2.002(2)	1.348(2)	1.383(2)	1.414(2)	1.398(2)	1.397(2)	2.133(2)
	2.060(2)	2.020(2)		1.393(2)	1.407(2)	1.416(2)	1.400(2)	
1-PMe$_2$Ph[c]	2.016(2)	2.014(2)	1.349(2)	1.385(2)	1.407(2)	1.415(2)	1.394(2)	2.131(2)
	2.056(2)	2.016(2)		1.392(2)	1.404(2)	1.419(2)	1.403(2)	
1-(CNMe)$_2$[c]	2.019(2)	2.003(2)	1.338(3)	1.379(3)	1.411(3)	1.413(3)	1.396(3)	2.605(2)
	2.033(2)	2.009(2)		1.381(3)	1.406(3)	1.408(3)	1.396(3)	
1-L$_x$ (avg)[d]	2.033(2)	2.064(2)	1.350(3)	1.373(2)	1.396(2)	1.418(3)	1.403(2)	2.236(2)
	2.035(2)	2.068(2)		1.371(2)	1.395(2)	1.423(2)	1.401(2)	2.248(2)
2═NAd[b]	2.032(19)	2.022(24)	1.346(5)	1.381(8)	1.406(8)	1.413(7)	1.397(4)	
	2.172(5)	2.122(5)	1.436(8)	1.297(8)	1.373(7)	1.413(8)	1.389(8)	1.702(5)
2═O[c]	2.193(5)	2.084(5)		1.293(7)	1.384(8)	1.425(8)	1.402(7)	
	2.166(5)	2.074(5)	1.428(9)	1.303(8)	1.374(7)	1.420(8)	1.386(8)	1.702(5)
2═X (avg)[e]	2.200(5)	2.121(5)		1.300(8)	1.375(7)	1.418(8)	1.376(8)	
	2.160(2)	2.054(2)	1.433(2)	1.297(2)	1.377(2)	1.419(2)	1.395(2)	1.636(2)
	2.194(2)	2.064(2)		1.301(2)	1.375(2)	1.418(2)	1.388(2)	
	2.181(17)	2.087(29)	1.432(4)	1.299(4)	1.376(4)	1.419(4)	1.389(9)	

[a]All distances given to the thousandth place for ready comparison. [b]Two molecules per asymmetric unit. [c]Ref 2. [d]Average of all {(dadi)$^{4-}$}TiL$_x$ (1-L$_x$) distances. [e]Average of all {(dadi)$^{2-}$}Ti═X (**2**═X) distances.

between **1**-H·Li and a potential η^1-AlH_4 complex, the ^{7}Li NMR spectrum was taken, revealing a clear doublet at δ −0.27 with the requisite 11.3 Hz coupling. The ^{1}H NMR spectrum of **1**-H·Li also reveals typical aspects of the (dadi)Ti framework, including the aforementioned four Me doublets, differing methine resonances, and typical aromatic signals. In THF-d_8, the hydride collapses to a broad singlet ($\Delta\nu_{1/2} \sim 4$ Hz), which was absent in the ^{1}H NMR spectrum of the corresponding deuteride (**1**-D·Li). An absorption at 1800 cm^{-1} (ν(TiH)) is observed in the IR spectrum of **1**-H·Li, and while it was absent

DOI: 10.1021/acs.organomet.8b00188
Organometallics XXXX, XXX, XXX−XXX

in the corresponding **1**-D·Li IR spectrum, no clear ν(TiD) is evident, although subtle changes in the fingerprint region are seen around 1270 cm^{-1}, consistent with the deuteride. The hydride stretch of 1800 cm^{-1} is of high energy for an early metal but consistent with an anionic hydride that carries substantial charge.[7]

The coupling observed between the lithium and hydride nuclei in C_6D_6 suggests the lithium-hydride bond in [(dadi)-TiH][Li(THF)$_3$] (**1**-H·Li) has significant covalency. When dissolved in THF-d_8, the coupling is disrupted, prompting several explanations: (1) The rate of intermolecular lithium exchange is fast on the NMR spectroscopic time scale, effectively decoupling the hydride and lithium. (2) The lithium is solvated by THF but exists as a tight ion-pair. (3) THF completely solvates the lithium, separating it from the [(dadi)TiH]$^-$ anion. (4) ^{7}Li quadrupolar relaxation is unusually solvent-dependent.[36]

The many resonances attributable to (dadi)^n permit significant redundancy in the measurement of diffusion coefficients by the gradient method,[37,38] and these are listed along with average diffusion coefficients in Table 1. The ^{7}Li diffusion coefficients of 5.2(1) × 10^{-6} and 5.5(4) × 10^{-6} cm^2/sec in C_6D_6 and THF-d_8, respectively, do not differ significantly, suggesting the lithium is associated with the dadi complex in either solvent. Furthermore, the average diffusion coefficients for the dadi ligand of 4.1(2) × 10^{-6} and 5.0(5) × 10^{-6} cm^2/sec in C_6D_6 and THF-d_8, respectively, are on the same order of magnitude as those observed for the lithium, providing further evidence that it is associated with the dadi complex in THF solution. These observations are inconsistent with a fully solvated and separated Li$^+$(THF)$_n$ cation but are consistent with a tight ion pair or integral HLi bonding in THF but with fast exchange. If exchange is occurring in C_6D_6 solution, then it must be significantly slower in order for the J_{HLi} to be retained. Since **1**-H·Li exhibits a clean J_{LiH}, it is unlikely that quadrupolar relaxation is significant enough to be a factor in THF-d_8.

*2.1.5. Structure of [(dadi)TiCl][Li(THF)$_4$] (**1**-Cl·Li).* Dark green crystals were harvested from the metathesis procedure in Scheme 2, and a single crystal X-ray structure characterization (Table 2) revealed the chloride adduct, [(dadi)TiCl][Li-(THF)$_4$] (**1**-Cl·Li). The Li cation was coordinated by four THF molecules, and the [(dadi)TiCl] anion is roughly square pyramidal, as Figure 2 illustrates. Metric parameters for the chloride adduct are listed in Table 2 along with some comparative distances from related complexes. The N2−Ti−N3 "bite angle" is 73.55(15)°, while the imine-amide angles are 76.02(15) and 79.27(15)°, whose subtle variation reflects the skewed face-to-face orientation of the 2,6-^{i}Pr$_2$−C$_6$H$_3$ groups. The Ti is out of the imine-amide plane by ∼0.487 Å (∠N2−Ti−N4 = 140.75(15)°, ∠N1−Ti−N3 = 145.88(16)°), while the diamides are opened up relative to the other core angles at 117.33(14)°. The d(Ti−Cl) was 2.3104 Å, and the "imine" nitrogen−titanium bond lengths (d(TiN) = 1.999(4), 2.044(4) Å) were essentially identical to those of the amides (d(TiN) = 2.008(4), 2.018(4) Å), significant evidence that (dadi)$^{4-}$ is the redox state of the chelate. In corroboration, the CN(imine) distances are 1.371(6) and 1.382(6) Å, more appropriate for C−N single bonds, and d(C7−C8) = 1.343(7), a bond length closer to a carbon−carbon double bond.[39]

*2.1.6. Structure of [(dadi)TiCH$_3$][Li(THF)$_2$] (**1**-CH$_3$·Li).* Hydrocarbyl adducts of (dadi)Ti (**1**) crystallized as thin plates or were susceptible to solvent loss, but repeated efforts led to a successful X-ray structure determination of [(dadi)TiCH$_3$]-[Li(THF)$_2$] (**1**-CH$_3$·Li). One of two independent molecules of the methyl adduct is pictured in Figure 3, selected refinement details are given in the Supporting Information, and comparative metric parameters are listed in Table 2.

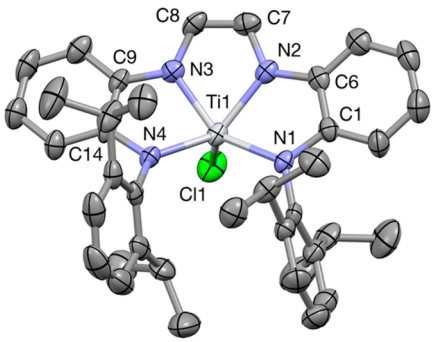

Figure 2. Molecular view of the anion pertaining to [(dadi)TiCl]-[Li(THF)$_4$] (**1**-Cl·Li). Table 2 contains selected distances, while its core angles (deg) are Cl−Ti−N1, 106.85(11); Cl−Ti−N2, 105.73(11); Cl−Ti−N3, 96.01(12); Cl−Ti−N4, 104.79(12); N1−Ti−N2, 76.02(15); N1−Ti−N3, 145.88(16); N1−Ti−N4, 117.33(14); N2−Ti−N3, 73.55(15); N2−Ti−N4, 140.75(15); N3−Ti−N4, 79.27(15).

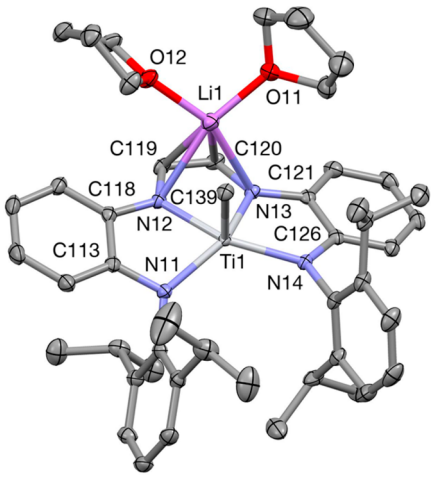

Figure 3. View of one of the two molecules of [(dadi)TiCH$_3$][Li-(THF)$_2$] (**1**-CH$_3$·Li) in the asymmetric unit. Table 2 contains selected average distances, while its average core angles (deg) are C−Ti−N(11,21), 97.03(5), 96.58(5); C−Ti−N(14,24), 103.33(5), 102.31(5); C−Ti−N(12,22), 94.73(5), 94.81(5); C−Ti−N(13,23), 110.03(5), 105.88(5); N(11,21)−Ti−N(12,22), 79.10(4), 78.74(4); N(11,21)−Ti−N(13,23), 141.73(4), 144.67(4); N(11,21)−Ti−N-(14,24), 123.94(4), 125.41(4); N(12,22)−Ti−N(13,23), 72.35(4), 72.60(4); N(12,22)−Ti−N(14,24), 147.70(4), 147.60(4); N-(13,23)−Ti−N(14,24), 76.35(4), 76.33(4).

1-CH$_3$·Li is a pseudosquare pyramidal species that has additional coordination to a Li(THF)$_2$ "cation" bound to the ene-diamide backbone of the dadi^{4-} ligand. The titanium is out of the N$_4$-plane by 0.384 (0.342) Å, and the resulting C−Ti−N angles are all >90°, with the methyl canted slightly toward the ene-diamide (95.8(12)° (avg)) backbone versus the arylamides (105.4(34)° (avg)). The bite angle of the ene-diamide averages 72.48(18)°, while the opposing angle between the arylamides averages 127.7(32)°. The remaining ene-amide/arylamide bite angles average 78.9(3) and 76.34(2)°.

DOI: 10.1021/acs.organomet.8b00188
Organometallics XXXX, XXX, XXX−XXX

Scheme 4. Imide Formation from RN_3 and Cyclopropanation of the dadi Backbone with $PhHCN_2$

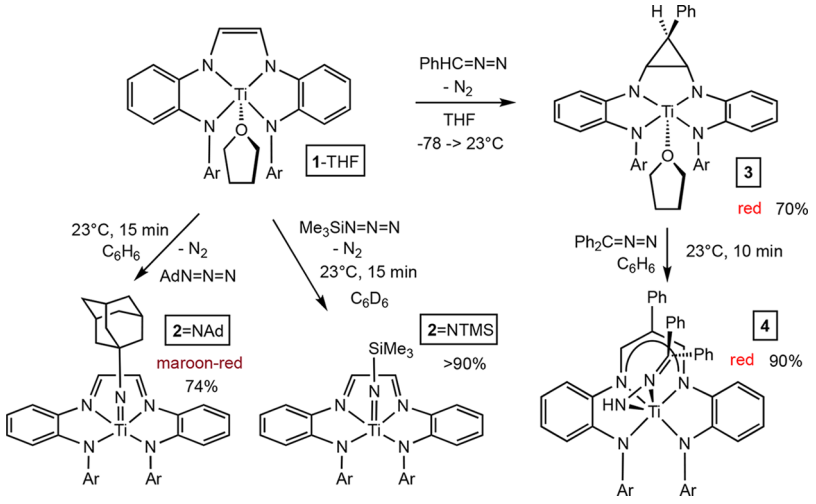

The titanium−carbon bond distance of 2.1318(16) Å (avg) is roughly equivalent to the sum of covalent radii (2.08 Å)[40] and the arylamide-titanium (2.012(8) Å (avg)), and ene-diamide-titanium bond lengths (2.019(4), 2.058(3) Å (avg)) are clearly both consistent with a tetraanionic $(dadi)^{4-}$ ligand. The average CN(imine) distance is 1.388(5) Å, consistent with C−N single bonds, and the average backbone CC bond length of 1.3487(6) Å is essentially a normal double bond distance.[39] The distinct molecules of **1**-CH_3·Li possess different d(C−Li) values (2.625(3), 2.421(3) Å), but both distances are substantially greater than the sum of covalent radii (2.00 Å), yet well within the sum of the van der Waals radii (~3.5 Å). The lithium appears to be loosely bound to the ene-diamide nitrogens and carbons at 2.417(36) (avg) and 2.387(36) (avg) Å, respectively, along with typical lithium−oxygen interactions from the THF at 1.934(17) Å (avg).

2.2. RN_3, $RCHN_2$ and (dadi)Ti(THF) (1-THF). *2.2.1. Synthesis of (dadi)Ti=NAd (2=NAd).* Unlike the treatment of (dadi)M (M = Fe, Cr(THF)) with organoazides,[3−6] which resulted in the nitrene insertions described in Scheme 1,[1] exposure of (dadi)Ti(THF) (**1**-THF) to stoichiometric amounts of AdN_3 permitted isolation of maroon-red (dadi)-Ti=NAd (**2**=NAd), as previously reported (Scheme 4).[2] The reaction of **1**-THF was essentially immediate in benzene, and **2**=NAd was reproducibly prepared in yields >70%. An NMR tube experiment with $TMSN_3$ cleanly produced a material (>90%) consistent with the imide (dadi)Ti=NTMS (**2**=NTMS), but the addition of 2,6-^{i}Pr$_2$−$C_6H_3N_3$ to **1**-THF produced a complicated product containing multiple isopropyl groups, indicative of a complex lacking any mirror symmetry.

2.2.2. Structure of (dadi)Ti=NAd (2=NAd). A single crystal X-ray structural determination of (dadi)Ti=NAd (**2**=NAd) was conducted, and even though the data set was twinned, it was refined to the extent that the imide structure consistent with previous NMR spectroscopic characterization was confirmed. A molecular view, showing the Ti roughly 0.53 Å above the N_4 plane, is given in Figure 4. The d(Ti=N) was 1.702(5) Å (avg), a typical value for Ti(IV) imides,[5,6,41] and the diimine titanium−nitrogen distances of 2.183(17) Å (avg) are somewhat longer than the amide Ti−N bond lengths of 2.100(25) (avg). This disparity is in line with the $(dadi)^{2-}$ formalism and stands in contrast to the nearly equal values attributable to d(TiN) in $(dadi)^{4-}$ (Table 2). Most importantly, the d(C=N) distances are appropriate for double bonds at 1.300(6) Å (avg), while the d(CC) of the dadi backbone is clearly a single bond distance (1.437(3) Å (avg)).[39]

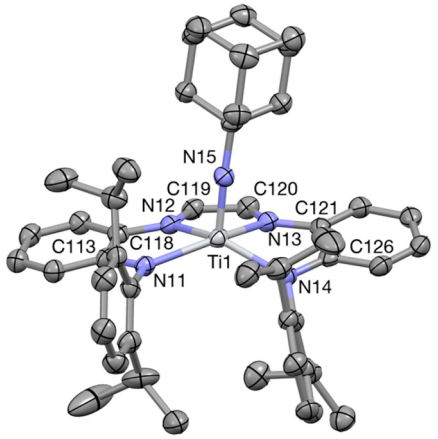

Figure 4. View of one of two (dadi)Ti=NAd (**2**=NAd) molecules in the asymmetric unit. Table 2 contains selected average distances, while its average core angles (deg) are N=Ti−N(11,21), 108.4(2), 108.1(2); N=Ti−N(14,24), 108.8(2), 108.7(2); N=Ti−N(12,22), 99.2(2), 91.7(2); N=Ti−N(13,23), 91.1(2), 100.0(3); N(11,21)−Ti−N(12,22), 75.52(18), 74.75(18); N(11,21)−Ti−N(13,23), 143.51(19), 136.08(19); N(11,21)−Ti−N(14,24), 123.73(19), 123.76(19); N(12,22)−Ti−N(13,23), 71.01(18), 71.37(19); N-(12,22)−Ti−N(14,24), 135.79(19), 143.18(19); N(13,23)−Ti−N-(14,24), 74.85(19), 74.99(19).

2.2.3. Cyclopropanation of $dadi^{4-}$. The generation of (dadi)Ti=NAd (**2**=NAd) suggested that titanium alkylidenes[42−55] can be similarly formed via diazoalkanes.[24−33] After attempts at protonation[56] of (dadi)Ti(CH=CH_2)·Li-$(THF)_{3-4}$ (**1**-CH=CH_2·Li) and hydride abstraction from (dadi)Ti(CH_3)·Li$(THF)_2$ (**1**-CH_3·Li) failed to elicit the desired (dadi)Ti=CHR (R = Me, H), a conventional route via diazoalkanes was attempted. As previously stated, Ph_2CN_2 simply produced the aforementioned adduct,[34] (dadi)Ti(N=N=CPh_2) (**1**-NNCPh_2), but use of $PhHCN_2$ generated a red complex with a cyclopropanated[9,10] backbone, {PhC_3H_3-$(NC_6H_4$-2-NAr$)_2$}Ti(THF) (**3**, Ar = 2,6-^{i}Pr$_2$−C_6H_3), in 70% yield (Scheme 4).

DOI: 10.1021/acs.organomet.8b00188
Organometallics XXXX, XXX, XXX−XXX

The observation of a mirror plane and resonances consistent with 5-coordination in the ^{1}H NMR spectrum of **3** were puzzling in view of its assimilation of $PhHCN_2$ and retention of THF. It appeared that the carbene fragment, PhHC:, had been incorporated into the dadi ligand and was not simply attached to titanium. An attempt was made to detect a plausible $PhHCN_2$ adduct, or other intermediate, by variable temperature ^{1}H NMR spectroscopy, but broad, unchanging resonances observed between −100 and −80 °C in THF-d_8 were not decipherable. Upon warming to −65 °C, broad resonances were still observed, and about 60% conversion to product $\{PhC_3H_3$-$(NC_6H_4$-2-$NAr)_2\}Ti(THF)$ (**3**) was apparent, consistent with a barrier to cyclopropanation of ∼15 kcal/mol. Further warming to −55 °C revealed total conversion, and one dominant isomer was produced (>95%) according to ^{1}H NMR spectroscopy. Direct cyclopropanation of the $(dadi)^{4-}$ ligand, without $PhHCN_2$ binding to the metal, was calculated to have a barrier incommensurate with the observed rate.

*2.2.4. Structure of {PhC$_3$H$_3$-2,3-NC$_6$H$_4$-2-Ar)}Ti(THF) (**3**).* Figure 5 illustrates a molecular view of 5-coordinate

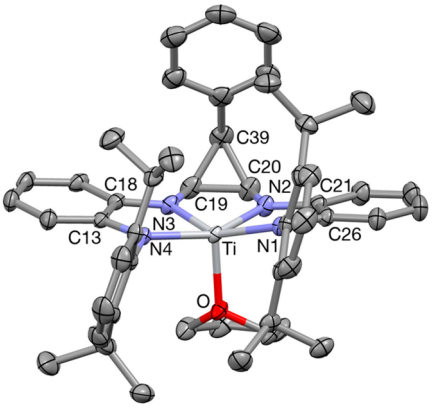

Figure 5. Molecular view of $\{PhC_3H_3(-NC_6H_4$-2-$Ar)_2\}Ti(THF)$ (**3**, Ar = 2,6-^{i}Pr$_2$). Selected interatomic distances (Å) and angles (deg): Ti−O, 2.0796(9); Ti−N1, 2.0228(10); Ti−N2, 1.9892(11); Ti−N3, 1.9915(10); Ti−N4, 2.0089(10); N3−C19, 1.4364(17); N2−C20, 1.4292(17); C19−C20, 1.495(2); C19−C39, 1.518(2); C20−C39, 1.518(2); O−Ti−N1, 104.94(4); O−Ti−N2, 93.64(4); O−Ti−N3, 96.83(4); O−Ti−N4, 100.32(4); N1−Ti−N2, 78.85(4); N1−Ti−N3, 147.35(5); N1−Ti−N4, 120.63(4); N2−Ti−N3, 75.72(4); N2−Ti−N4, 151.29(4); N3−Ti−N4, 77.78(4).

$\{PhC_3H_3(-NC_6H_4$-2-$NAr)_2\}Ti(THF)$ (**3**, Ar = 2,6-^{i}Pr$_2$−C_6H_3), showing that the $(CH)_2N_2$ backbone of the $(dadi)^{4-}$ ligand was cyclopropanated, yielding a product with the phenyl group oriented toward the titanium core, and the proton of the "carbene" directed away. The titanium−nitrogen distances average 2.003(16) Å and can be all be assigned as amide linkages. The titanium is slightly out of the N_4-amide plane (0.3 Å), as the O−Ti−N angles are >90°, and the THF is oriented away from the aryl amides (O−Ti−N1/N4 = 104.94(4)/100.32(4)), presumably due to sterics. All distances and angles are appropriate for the cyclopropane unit, and the remainder of the tetradentate chelate is similar to that of $(dadi)^n$. Aryldiamide bite angles of 78.85(4) and 77.78(4)° are accompanied by the backbone diimine bite angle of 75.72(4)°, leaving the usual open arylamide−titanium−arylamide angle of 120.63(4)°.

2.2.5. Nacnac Formation. The formation of a cyclopropanated backbone of $(dadi)^n$ suggested that reversible C−C bond formation could be a means of storing and releasing electrons in a redox noninnocent (RNI) fashion.[12,57−67] A possible hindrance to RNI is the transfer of a cyclopropane hydrogen subsequent to ring-opening, which would generate a nacnac fragment in place of the original diimine. The reactivity of $\{PhC_3H_3(-NC_6H_4$-2-$NAr)_2\}Ti(THF)$ (**3**) was probed via various potential oxidants and proton acceptors, and while most generated mixtures, the addition of Ph_2CN_2 yielded a single product (>90%) that was dissymmetric. ^{1}H NMR spectroscopic resonances that revealed the loss of a cyclopropane hydrogen, and a ν(NH) at 3303 cm^{-1} in its IR spectrum, were consistent with the generation of a nacnac tetradentate chelate,[13,62] $\{PhC(CHNC_6H_4$-2-$NAr)_2\}Ti(\eta^2$-$HNNCPh_2)$ (**4**, Ar = 2,6-^{i}Pr$_2$−C_6H_3). Despite the exo-regiochemistry of the cyclopropane β-hydrogen, transfer to the α-nitrogen of coordinated Ph_2CN_2 occurs, perhaps subsequent to ring opening, to generate the trianionic $\{PhC(CHNC_6H_4$-2-$NAr)_2\}^{3-}$ ligand. The chemistry provides a blueprint to how reversible C−C bond formation can be utilized in a redox noninnocent fashion, but it is likely that the β-carbon of the cyclopropane unit will need to have two non-hydrogen substituents.[63]

*2.2.6. Structure of {PhC(CHNC$_6$H$_4$-2-NAr)$_2$}Ti(η^2-HNNCPh$_2$) (**4**).* Pictured in Figure 6 is a molecular view of {PhC-

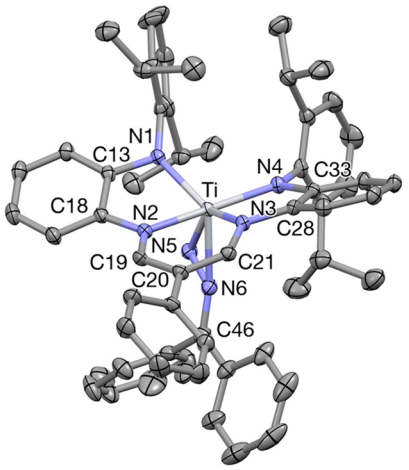

Figure 6. Molecular view of $\{PhC(CHNC_6H_4$-2-$NAr)_2\}Ti(\eta^2$-$HNNCPh_2)$ (**4**, Ar = 2,6-^{i}Pr$_2$−C_6H_3, Scheme 4). Selected interatomic distances (Å) and angles (deg): Ti−N1, 2.0023(12); Ti−N2, 2.1316(12); Ti−N3, 2.1389(12); Ti−N4, 2.0115(12); Ti−N5, 1.9243(13); Ti−N6, 2.1899(13); N2−C19, 1.3288(18); C19−C20, 1.389(2); C20−C21, 1.393(2); N3−C21, 1.3322(18); N1−Ti−N2, 78.00(5); N1−Ti−N3, 129.24(5); N1−Ti−N4, 111.13(5); N1−Ti−N5, 92.67(5); N1−Ti−N6, 126.72(5); N2−Ti−N3, 79.83(4); N2−Ti−N4, 156.03(5); N2−Ti−N5, 92.95(5); N2−Ti−N6, 85.43(5); N3−Ti−N4, 77.42(4); N3−Ti−N5, 133.64(5); N3−Ti−N6, 95.96(5); N4−Ti−N5, 108.23(5); N4−Ti−N6, 104.32(5); N5−Ti−N6, 37.68(5).

$(CHNC_6H_4$-2-$NAr)_2\}Ti(\eta^2$-$HNNCPh_2)$ (**4**, Ar = 2,6-^{i}Pr$_2$) that reveals the asymmetry in the compound evident by NMR spectroscopy. The nacnac portion of the ligand is characterized by d(Ti−N) of 2.1316(12) and 2.1389(12) Å, while the titanium-amide nitrogen distances are normal (Ti−N1, 2.0023(12); Ti−N4, 2.0115(12)). The η^2-$HNNCPh_2$ linkage is angled across the face of the nacnac-diarylamide titanium

DOI: 10.1021/acs.organomet.8b00188
Organometallics XXXX, XXX, XXX−XXX

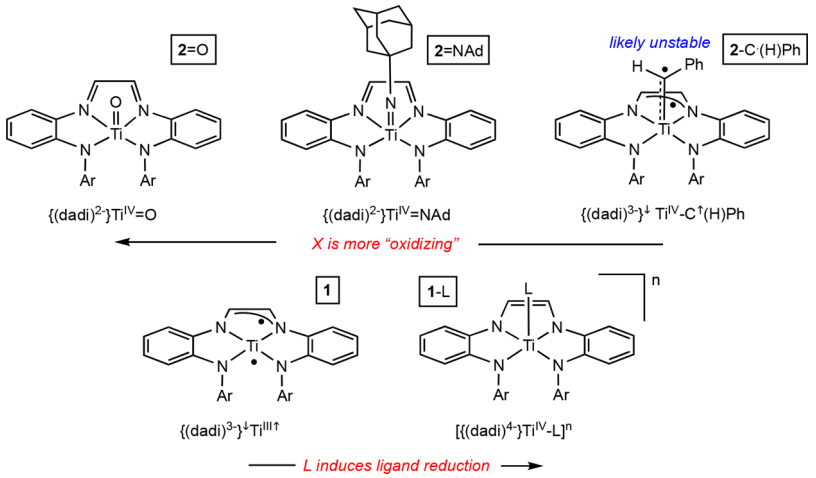

Figure 7. Progressively more oxidizing X, O > NAd > CHPh, and the dadi redox consequences compared to that of calculated $\{(dadi)^{\cdot\uparrow}\}^{3-}Ti^{III}\downarrow$ (**1**) and adducts $[\{(dadi)^{4-}\}Ti^{IV}\text{-}L]^{n}$ (**1**-L).

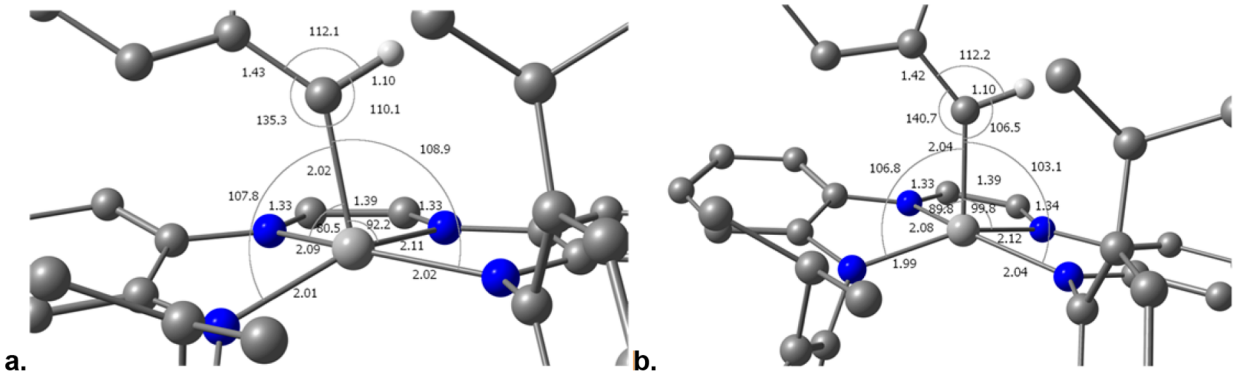

Figure 8. Geometries of unrestricted singlet (0.0 kcal/mol; a) and unrestricted triplet (3.4 kcal/mol; b) DFT (ONIOM(M06/6-311+G(d):UFF) calculations of (dadi)TiC(H)Ph (**2**-C·HPh). The restricted singlet (0.5 kcal/mol) is not shown but similar to panel a.

core such that the mirror symmetry is broken. Its amide d(TiN) is 1.9243(13) Å, and its titanium−β-N distance is considerably longer at 2.1899(13) Å, although clearly within reason for a simple donor interaction. The remaining distances and angles, a selected group of which are indicated in the caption of Figure 6, are as expected for this low symmetry complex.

3. DISCUSSION

3.1. Redox Parameters of $[(dadi)^{n}Ti(=X/L)]^{n}$. The metric parameters in Table 2 unquestionably show two discrete states of $(dadi)^{n}$ are $n = -2$ for (dadi)Ti = X (**2**═X) species and $n = -4$ for adducts (dadi)TiL (**1**-L). In order to generate $(dadi)^{2-}$, the ligand(s) X or L need to be oxidizing enough to pull 2 electrons out of $(dadi)^{4-}$. As previously discussed, even a ligand with significant backbonding capability, such as CO or CNR,[2] does not convert the $(dadi)^{n}$ from $n = -4$ to $n = -2$. In the case of azide RN_3, a nitrene precursor, the RN generated via N_2 loss is a potent enough oxidant to generate RN^{2-} by oxidizing the $dadi^{4-}$. It is interesting that the titanium does not change its formal oxidation state,[7] as the ligands are far more redox active and incur all the redox changes. Nitrene insertions into the dadi backbone of the Fe and Cr species illustrated in Scheme 1 occur because RN does not have the oxidizing power in these systems to fully convert the metal to M(IV). As a consequence, nitrene or imidyl (M(III)) chemistry rather than imide chemistry is observed.

Attempts to generate (dadi)Ti═CRR′ have failed, and according to calculations, the generation of a stable alkylidene may not be possible since the RR′C: fragment is not oxidizing enough to pull electrons from $(dadi)^{4-}$. As indicated in Figure 7., calculations on a benzylidene portray it as a diradical species[66,67] best considered $(dadi\cdot^{\uparrow})^{3-}Ti^{IV}(C\cdot^{\downarrow}$ (H)Ph) (**2**-C·HPh). Figure 8 illustrates the calculated geometries of **2**-C·HPh which show the $d(CN_{im})$ to be 1.33 Å, and d(CC) = 1.39 Å, values that are *between* those found for dianionic ($n = -2$) and tetraanionic ($n = -4$) forms of $(dadi)^{n}$. The d(TiC) of 2.02 Å in the singlet geometries is consistent with a double bond, but the ligand metrics force one to conclude that unpaired spin density on $(dadi\cdot)^{3-}$ is likely antiferromagnetically coupled to a radical benzylidene anion $(:C\cdot PhH)^{-}$. The triplet version, having the $(dadi\cdot)^{3-}$ ferromagnetically coupled to the $(:C\cdot PhH)^{-}$, is only 3.4 kcal/mol above the singlet.

Previous calculations on (dadi)Ti (**1**), a species that has not been isolated or observed with confidence, have shown it to be best construed as $\{(dadi)^{3-}\}^{\downarrow}Ti^{III}\uparrow$, where the electron on titanium is antiferromagnetically coupled to an odd electron on the $dadi^{3-}$ ligand. The donation of any L to **1**, even a weak ligand such as THF, increases the electron density at the metal and causes the transfer of another electron to $(dadi)^{4-}$; hence, all (dadi)TiL (**1**-L) are $\{(dadi)^{4-}\}Ti^{IV}$-L.

Figure 9 illustrates a truncated molecular orbital diagram of (dadi)Ti(THF) (**1**-THF), showing a 2.85 eV gap between the HOMO, an orbital with backbone carbon−carbon double

DOI: 10.1021/acs.organomet.8b00188
Organometallics XXXX, XXX, XXX−XXX

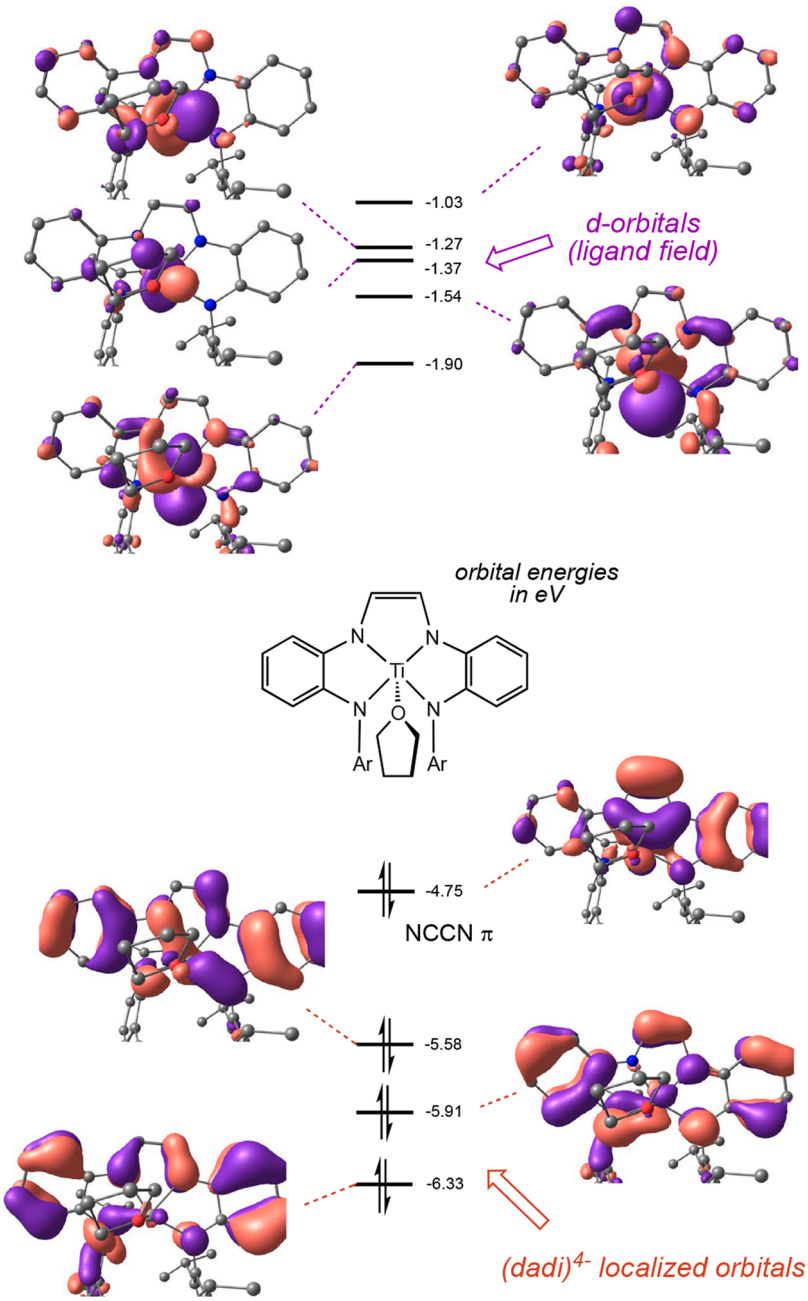

Figure 9. Truncated molecular orbital diagram of (dadi)Ti(THF) (**1**-THF), showing empty d-orbitals (M06/6-311+G(d) orbital energies at the ONIOM(M06/6-311+G(d):UFF) optimized minimum of singlet **1**-THF), and the four, highest occupied $(dadi)^{4-}$ molecular orbitals.

bond and diamide character, and the LUMO, a d-orbital of roughly *xy*-character. It is also clear that the empty d-orbitals, which span only 0.87 eV, reflect the low symmetry of the system and are difficult to assign. The HOMO is 0.83 eV above the HOMO−1, an orbital that has most of its spin density on the aryl rings. In general, the MO diagram is quite similar to that of (dadi)Ti(PMe_2Ph) (**1**-PMe_2Ph),[2] which has a HOMO/LUMO gap of 2.96 eV, and a 0.85 eV gap between its HOMO and HOMO−1. Both MO diagrams are consistent with a $(dadi)^{4-}$ redox state of the chelate, and both show the HOMO to be the same NCCNπ orbital that clearly indicated C═C double bond character.

Evidence of intimate lithium bonding in the case of [(dadi)TiCCPh][$Li(THF)_2$] (**1**-CCPh·Li) stems from the observation of J_{CLi}, while gradient diffusion experiments in addition to lithium-hydride coupling support the contention that Li may be directly bound in [(dadi)TiH][$Li(THF)_{3-5}$] (**1**-H·Li). Figure 10 illustrates potential structures of these

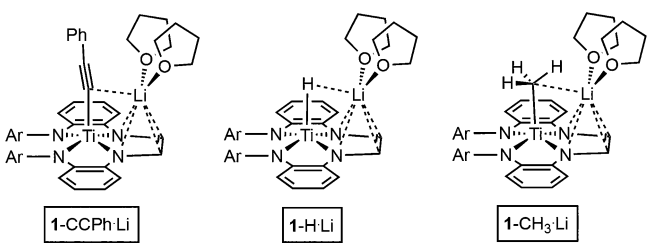

Figure 10. Plausible structures of complexes exhibiting J_{LiH} based on the crystal structure of [(dadi)$TiCH_3$][$Li(THF)_2$] (**1**-CH_3·Li).

DOI: 10.1021/acs.organomet.8b00188
Organometallics XXXX, XXX, XXX−XXX

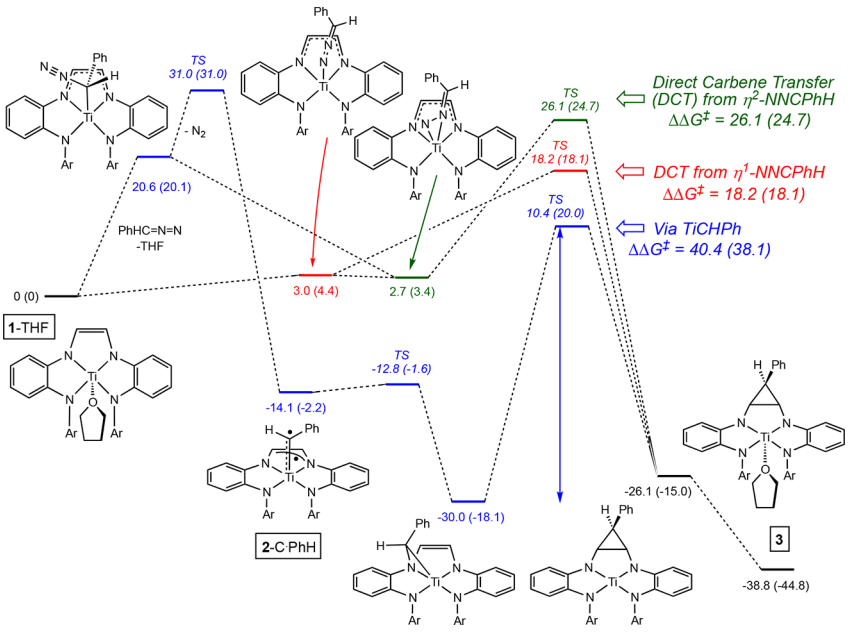

Figure 11. Computed intermediates ($\Delta G°$ ($\Delta H°$)) relative to (dadi)Ti(THF) (**1**) in three cyclopropanation mechanisms. A "direct carbene transfer" to the dadi backbone possesses a lower barrier than one involving the intermediacy of (dadi)TiCHPh, and it is likely to occur via an η^1-NNCPhH. The product with opposite cyclopropane stereochemistry has a lower free energy of −40.7 kcal/mol ($\Delta H°$ = −44.0 kcal/mol). Calculations at the M06/6-311+G(d)/ONIOM(M06/6-311+G(d):UFF level.

species based on the X-ray crystal structure of [(dadi)TiCH$_3$]-[Li(THF)$_2$] (**1**-CH$_3$·Li, Figure 3). While the alkyl complexes [(dadi)TiR][Li(THF)$_2$] (**1**-R·Li, R = Me, ^{neo}Pe) do not manifest lithium−hydrogen coupling, it may be that the sp^3 and sp^2 (e.g., [(dadi)TiCH═CH$_2$][Li(THF)$_2$] (**1**-CH═CH$_2$·Li)) constituents lack the appropriate orbital overlap for significant interaction. The crystal structure in Figure 2 supports a modest CH$_3$···Li contact, and the s- and sp-interactions of the hydride **1**-H·Li and acetylide **1**-CCPh·Li complexes, respectively, are likely to permit enough orbital overlap for $J_{Li(C/H)}$ to be observed.

3.2. Mechanism of the Cyclopropanation of (dadi)Ti-(THF) (1-THF). The mechanism of the dadi cyclopropanation revealed in Scheme 4 was assumed to occur via the generation of (dadi)TiCHPh, but calculations invoke a different process. First, exogenous cyclopropanation of the dadi ligand by PhHCN$_2$ does not appear feasible, as the 1,3-dipolar addition mechanism[68] was calculated to have a barrier of $\Delta G^‡$ = 50.4 kcal/mol ($\Delta H^‡$ = 53.7 kcal/mol). Figure 11 illustrates three plausible mechanisms initiated by binding of PhHCN$_2$ to titanium, which is slightly unfavorable for both the η^1- (3.0 kcal/mol, red) and η^2-NNCHPh (2.7 kcal/mol, green) species and significantly unfavorable for the carbon-bound η^1−C-N$_2$CPhH adduct (20.6 kcal/mol). Two paths refer to direct cyclopropanation (direct carbene transfer) from the diazoalkane adducts to the dadi ligand, and the third involves the intermediacy of the titanium alkylidene (via TiCHPh, blue). The calculations support direct cyclopropanation from the η^1-N$_2$CHPh adduct, as its $\Delta G^‡$ of 18.2 kcal/mol ($\Delta H^‡$ = 18.1 kcal/mol) is reasonably close to the crude experimental barrier of ∼15 kcal/mol.

While the transfer of PhHC: to titanium is more favorable ($\Delta G°$ = −14.1 kcal/mol), a considerable barrier is found ($\Delta G^‡$ = 31.0 kcal/mol) for dinitrogen loss via the unfavorable η^1-C−N$_2$CPhH adduct at 20.6 kcal/mol to form (dadi·$^{↑}$)^3−Ti^{IV}(C·$^{↓}$(H)Ph) (**2**-C·(H)Ph). More importantly, formation of a titanaaziridine ensues via attack at an imine nitrogen, and it is considerably stable at $\Delta G°$ = −30.0 kcal/mol. The barrier to cyclopropanation via the titanaaziridine (via TiCHPh), which is a two-step process, is quite substantial at $\Delta G^‡$ = 40.4 kcal/mol ($\Delta H^‡$ = 38.1 kcal/mol). It appears likely that sterics impact the ability of PhHCN$_2$ to transfer PhHC: to the titanium; otherwise, the titanaaziridene might be a free energy sink in the system, as the benzylidene radical (**2**-C·(H)Ph) is not likely to be a stable species. In contrast, the simple η^1-NNCHPh adduct is ideally positioned above the dadi backbone for carbene transfer, and it is the clear path of choice. Note that this cyclopropanation contrasts with the nitrene mediated aziridination of the dadi ligand illustrated in Scheme 1.

The generally accepted mechanism for transition-metal-catalyzed cyclopropanations derived from diazoalkanes assumes the transfer of the carbene fragment to the metal prior to its transfer to substrate.[32] Little mechanistic work has been done on the process, likely due to the lack of observable intermediates, aside from the elegant spectroscopic study by Berry and Lancaster pertaining to dirhodium-catalyzed cyclopropanations.[69] While the chemistry described herein is intramolecular, it does suggest that concluding alkylidenes must be intermediates in cyclopropanation may not be wise, especially in instances where potent Lewis acidic centers are involved. Note that Mindiola has recently shown that alkylidene formation from Ph$_3$PCH$_2$ is productive in promoting alkane dehydrogenation via methylene transfer to Ti(II), so titanium alkylidenes can form via a standard oxidation path.[70] In the (dadi)Ti system, titanium alkylidenes do not have similar stabilities.

4. CONCLUSIONS

The formation of adducts [(dadi)Ti(L/X)]^m (**1**-L, m = 0, N$_2$CPh$_2$; m = −1, X = Cl$^−$, N$_3^−$, O^{i}Pr$^−$, CH$_3^−$, ^{neo}Pe$^−$, CH═CH$_2^−$, CCPh$^−$, CCTMS$^−$, H(D)$^−$) were prepared via L or X$^−$

DOI: 10.1021/acs.organomet.8b00188
Organometallics XXXX, XXX, XXX−XXX

addition to (dadi)Ti(THF) (**1**-THF). No donor has proven to be "oxidizing" enough to extract electron density from the $dadi^{4-}$ ligand. Previous work established that PR_3 and CNR led to Ti(IV) species,[2] and all of the donors utilized herein generate $[\{(dadi)^{4-}\}Ti^{IV}(L/X)]^n$, although structural evidence was obtained for only **1**-Cl·Li and **1**-CH_3. Even when potential $2e^-$ oxidants are added, redox changes at the ligand are difficult to realize. Organoazides AdN_3 and Me_3SiN_3 led to the formation of imide species (dadi)Ti═NR (**2**═NR, R = Ad, $SiMe_3$), and the structure of **2**═NAd clearly shows oxidation of the ligand to $(dadi)^{2-}$. In contrast, attempts to prepare alkylidenes in a related fashion from Ph_2CN_2 and $PhHCN_2$ failed to yield the desired (dadi)Ti═CHRR′ species.

In the case of $PhHCN_2$, its addition to (dadi)Ti(THF) (**1**-THF) afforded $\{PhC_3H_3(\text{-}NC_6H_4\text{-}2\text{-}NAr)_2\}$Ti(THF) (**3**), a complex in which the C═C bond in the backbone of $(dadi)^{4-}$ was cyclopropanated. Initially, this reaction appeared to be analogous to previous nitrene insertions, but calculations suggested the contrary. The reaction that would form an alkylidene upon dinitrogen extrusion was calculated to yield $(dadi^{\uparrow})^{3-}Ti^{IV}(C\cdot^{\downarrow}(H)Ph)$ (**2**-C·(H)Ph), a complex in which formation of a full titanium−carbon double bond is incomplete. The alkylidene is not a potent enough oxidant, and the chelate is in the $(dadi)^{3-}$ state, rendering **2**-C·(H)Ph highly reactive. It would be expected to immediately attack the "imine" nitrogen to generate a metallaaziridene, from which further reactivity has large activation energies. It is likely that N_2 loss only occurs after or during cyclopropanation, which is calculated to occur from an η^1-N_2CHPh adduct.

It was immediately recognized that reversible C−C bond formation from $\{PhC_3H_3(\text{-}NC_6H_4\text{-}2\text{-}NAr)_2\}$Ti(THF) (**3**) could be a means of electron storage, a different construct of redox noninnocence (RNI). In this case, the β-hydrogen on the cyclopropane ring of **3** has proven to be a hindrance, as indicated by treatment of the compound with Ph_2CN_2, which yielded a nacnac derivative, $\{PhC(CHNC_6H_4\text{-}2\text{-}NAr)_2\}$Ti($\eta^2$-$HNNCPh_2$) (**4**), upon hydrogen transfer. Construction of ligand systems capable of RNI via reversible C−C bond formation is now being sought through application of related chelates with two constituents in the β-position.

5. EXPERIMENTAL SECTION

Full experimental details are given in the Supporting Information, including gradient diffusion plots, X-ray crystal structure information, computational procedures, synthetic procedures, and spectra. Qualitative descriptions of the synthetic experiments and crystallographic data collection and refinements are given in the schemes, figures, and tables.

■ ASSOCIATED CONTENT

Supporting Information

The Supporting Information is available free of charge on the ACS Publications website at DOI: 10.1021/acs.organomet.8b00188.

Gradient diffusion plots, X-ray crystal structure information, computational procedures, synthetic procedures, and spectra (PDF)

Accession Codes

CCDC 1836208−1836212 contain the supplementary crystallographic data for this paper. These data can be obtained free of charge via www.ccdc.cam.ac.uk/data_request/cif, or by emailing data_request@ccdc.cam.ac.uk, or by contacting The Cambridge Crystallographic Data Centre, 12 Union Road, Cambridge CB2 1EZ, UK; fax: +44 1223 336033.

■ AUTHOR INFORMATION

Corresponding Author

*Tel.: 607-255-7220. E-mail: ptw2@cornell.edu.

ORCID

Thomas R. Cundari: 0000-0003-1822-6473

Peter T. Wolczanski: 0000-0003-4801-0614

Notes

The authors declare no competing financial interest.

■ ACKNOWLEDGMENTS

Support from the National Science Foundation (CHE-1402149; CHE-1664580) and Cornell University is gratefully acknowledged, as is the U.S. Department of Energy, Office of Basic Energy Sciences for partial support of this research (TRC, DE-FG02-03ER15387). NSF support for the CCB NMR facility (NSF-MRI CHE-1531632) is appreciated, as is technical aid from Ivan Keresztes. We thank Bufan Zhang for analytical support. This paper is dedicated to Ernesto Carmona (University of Seville), whose research in organometallic chemistry, especially metal−carbon double bonds, serves as inspiration for parts of this work.

■ REFERENCES

(1) Heins, S. P.; Morris, W. D.; Wolczanski, P. T.; Lobkovsky, E. B.; Cundari, T. R. Nitrene Insertion into CC and CH Bonds of Diamide-diimine Ligated Chromium and Iron Complexes. *Angew. Chem., Int. Ed.* **2015**, *54*, 14407−14411.

(2) Heins, S. P.; Wolczanski, P. T.; Cundari, T. R.; MacMillan, S. N. Redox non-innocence permits catalytic nitrene carbonylation by (dadi)Ti═NAd (Ad = adamantyl). *Chem. Sci.* **2017**, *8*, 3410−3418.

(3) Katsuki, T. Azide compounds: Nitrogen sources for atom-efficient and ecologically benign nitrogen-atom-transfer reactions. *Chem. Lett.* **2005**, *34*, 1304−1309.

(4) Huang, X. Y.; Bergsten, T. M.; Groves, J. T. Manganese-Catalyzed Late-Stage Aliphatic C-H Azidation. *J. Am. Chem. Soc.* **2015**, *137*, 5300−5303.

(5) Wigley, D. E.; Karlin, K. D. Organoimido Complexes of the Transition-metals. *Prog. Inorg. Chem.* **1994**, *42*, 239−482.

(6) Nugent, W. A.; Mayer, J. M. *Metal−Ligand Multiple Bonds*; Wiley-Interscience: New York, 1988.

(7) Wolczanski, P. T. Flipping the Oxidation State Formalism: Charge Distribution in Organometallic Complexes as Reported by Carbon Monoxide. *Organometallics* **2017**, *36*, 622−631.

(8) (a) Peloso, R.; Carmona, E. Non-heteroatom-substituted alkylidene complexes of groups 10 and 11. *Coord. Chem. Rev.* **2018**, *355*, 116−132. (b) Schrock, R. R. High Oxidation State Multiple Metal-carbon Bonds. *Chem. Rev.* **2002**, *102*, 145−179. (c) Vougioukalakis, G. C.; Grubbs, R. H. Ruthenium-based Heterocyclic Carbene-coordinated Olefin Metathesis Catalysts. *Chem. Rev.* **2010**, *110*, 1746−1787. (d) Esteruelas, M. A.; Lopez, A. M.; Olivan, M. Osmium-carbon double bonds: Formation and reactions. *Coord. Chem. Rev.* **2007**, *251*, 795−840.

(9) (a) Bruckner, R. *Organic Mechanisms*; Harmata, M., Ed.; Springer: Berlin, 2010. (b) Candeias, N. R.; Afonso, C. A. M. Developments in the Photochemistry of Diazo Compounds. *Curr. Org. Chem.* **2009**, *13*, 763−787. (c) Engel, P. S. Mechanism of the Thermal and Photochemical Decomposition of Azoalkanes. *Chem. Rev.* **1980**, *80*, 99−150. (d) Crawford, R. J.; Mishra, A. Mechanism of Thermal Decomposition of 1-Pyrazolines and Its Relationship to Cyclopropane Isomerizations. *J. Am. Chem. Soc.* **1966**, *88*, 3963−3969.

DOI: 10.1021/acs.organomet.8b00188
Organometallics XXXX, XXX, XXX−XXX

(10) (a) Levesque, E.; Goudreau, S. R.; Charette, A. B. Improved Zinc-Catalyzed Simmons-Smith Reaction: Access to Various 1,2,3-Trisubstituted Cyclopropanes. *Org. Lett.* **2014**, *16*, 1490−1493. (b) Creary, X. Tosylhydrazome Salt Pyrolyses: Phenyldiazomethanes. *Org. Synth.* **1986**, *64*, 207−216.
(11) Edema, J. J. H.; Duchateau, R.; Gambarotta, S.; Hynes, R.; Gabe, E. Novel Titanium(II) Amine Complexes L_4TiCl_2 [L = 1/2 N,N,N′,N′-Tetramethylethylenediamine (TMEDA), 1,2 N,N,N′-Trimethylethylenediamine, Pyridine, 1/2 2,2′-Bipyridine]: Synthesis and Crystal Structure of Monomeric *trans*-$(TMEDA)_2TiCl_2$. *Inorg. Chem.* **1991**, *30*, 154−156.
(12) Frazier, B. A.; Wolczanski, P. T.; Keresztes, I.; DeBeer, S.; Lobkovsky, E. B.; Pierpont, A. W.; Cundari, T. R. Synthetic Approaches to $(smif)_2Ti$ (smif = 1,3-di-(2-pyridyl)-2-azaallyl) Reveal Redox Non-Innocence and C-C Bond-Formation. *Inorg. Chem.* **2012**, *51*, 8177−8186.
(13) Williams, V. A.; Wolczanski, P. T.; Sutter, J.; Meyer, K.; Lobkovsky, E. B.; Cundari, T. R. Iron Complexes Derived from $\{nacnac\text{-}(CH_2py)_2\}^-$ and $\{nacnac\text{-}(CH_2py)(CHpy)\}^n$ Ligands: Stabilization of Fe(II) via Redox Non-innocence. *Inorg. Chem.* **2014**, *53*, 4459−4474.
(14) Vogel, C.; Heinemann, F. W.; Sutter, J.; Anthon, C.; Meyer, K. An iron nitride complex. *Angew. Chem., Int. Ed.* **2008**, *47*, 2681−2684.
(15) Sabenya, G.; Lazaro, L.; Gamba, I.; Martin-Diaconescu, V.; Andris, E.; Weyhermuller, T.; Neese, F.; Roithova, J.; Bill, E.; Lloret-Fillol, J.; Costas, M. Generation, Spectroscopic, and Chemical Characterization of an Octahedral Iron(V)-Nitrido Species with a Neutral Ligand Platform. *J. Am. Chem. Soc.* **2017**, *139*, 9168−9177.
(16) Walstrom, A.; Pink, M.; Yang, X.; Tomaszewski, J.; Baik, M.-H.; Caulton, K. G. A facile approach to a *d*(4) Ru═N: Moiety. *J. Am. Chem. Soc.* **2005**, *127*, 5330−5331.
(17) Maity, A. K.; Murillo, J.; Metta-Magana, A. J.; Pinter, B.; Fortier, S. A Terminal Iron(IV) Nitride Supported by a Super Bulky Guanidinate Ligand and Examination of Its Electronic Structure and Reactivity. *J. Am. Chem. Soc.* **2017**, *139*, 15691−15700.
(18) Schendzielorz, F. S.; Finger, M.; Volkmann, C.; Würtele, C.; Schneider, S. A Terminal Osmium(IV) Nitride: Ammonia Formation and Ambiphilic Reactivity. *Angew. Chem., Int. Ed.* **2016**, *55*, 11417−11420.
(19) (a) Scheibel, M. G.; Askevold, B.; Heinemann, F. W.; Reijerse, E. J.; de Bruin, B.; Schneider, S. Closed-shell and open-shell square-planar iridium nitrido complexes. *Nat. Chem.* **2012**, *4*, 552−555. (b) Scheibel, M. G.; Wu, Y. L.; Stuckl, A. C.; Krause, L.; Carl, E.; Stalke, D.; de Bruin, B.; Schneider, S. Synthesis and Reactivity of a Transient, Terminal Nitrido Complex of Rhodium. *J. Am. Chem. Soc.* **2013**, *135*, 17719−17722.
(20) Tran, B. L.; Krzystek, J.; Ozarowski, A.; Chen, C. H.; Pink, M.; Karty, J. A.; Telser, J.; Meyer, K.; Mindiola, D. J. Formation and Reactivity of the Terminal Vanadium Nitride Functionality. *Eur. J. Inorg. Chem.* **2013**, *2013*, 3916−3929.
(21) Atienza, C. C. H.; Bowman, A. C.; Lobkovsky, E.; Chirik, P. J. Photolysis and Thermolysis of Bis(imino)pyridine Cobalt Azides: C-H Activation from Putative Cobalt Nitrido Complexes. *J. Am. Chem. Soc.* **2010**, *132*, 16343−16345.
(22) Schöffel, J.; Rogachev, A. Y.; DeBeer George, S.; Burger, P. Isolation and Hydrogenation of a Complex with a Terminal Iridium-Nitrido Bond. *Angew. Chem., Int. Ed.* **2009**, *48*, 4734−4738.
(23) Berry, J. F.; Bill, E.; Bothe, E.; DeBeer George, S.; Mienert, B.; Neese, F.; Wiedhardt, K. An octahedral coordination complex of iron(VI). *Science* **2006**, *312*, 1937−1941.
(24) (a) Schwab, P.; Grubbs, R. H.; Ziller, J. W. Synthesis and applications of $RuCl_2(═CHR')(PR_3)_2$: The influence of the alkylidene moiety on metathesis activity. *J. Am. Chem. Soc.* **1996**, *118*, 100−110. (b) Schwab, P.; France, M. B.; Ziller, J. W.; Grubbs, R. H. A Series of Well-defined Metathesis Catalysts - Synthesis of $RuCl_2(═CHR')(PR_3)_2$ and Its Reactions. *Angew. Chem., Int. Ed. Engl.* **1995**, *34*, 2039−2041.
(25) Klose, A.; Solari, E.; Floriani, C.; Re, N.; Chiesi-Villa, A.; Rizzoli, C. Iron-carbene functionalities supported by a macrocyclic ligand: iron-carbon double bond stabilized by tetramethyldibenzotetraazaannulene. *Chem. Commun.* **1997**, 2297−2298.
(26) Esposito, V.; Solari, E.; Floriani, C.; Re, N.; Rizzoli, C.; Chiesi-Villa, A. Binding and redox properties of iron(II) bonded to an oxo surface modeled by calix[4]arene. *Inorg. Chem.* **2000**, *39*, 2604−2613.
(27) Li, Y.; Huang, J.-S.; Zhou, Z.-Y.; Che, C.-M.; You, X.-Z. Remarkably stable iron porphyrins bearing nonheteroatom-stabilized carbene or (Alkoxycarbonyl) carbenes: Isolation, X-ray crystal structures, and carbon atom transfer reactions with hydrocarbons. *J. Am. Chem. Soc.* **2002**, *124*, 13185−13193.
(28) (a) Russell, S. K.; Hoyt, J. M.; Bart, S. C.; Milsmann, C.; Stieber, S. C. E.; Semproni, S. P.; DeBeer, S.; Chirik, P. J. Synthesis, electronic structure and reactivity of bis(imino)pyridine iron carbene complexes: evidence for a carbene radical. *Chem. Sci.* **2014**, *5*, 1168−1174. (b) Russell, S. K.; Lobkovsky, E.; Chirik, P. J. N-N Bond Cleavage in Diazoalkanes by a Bis(imino)pyridine Iron Complex. *J. Am. Chem. Soc.* **2009**, *131*, 36−37.
(29) Iluc, V. M.; Hillhouse, G. L. Three-Coordinate Nickel Carbene Complexes and Their One-Electron Oxidation Products. *J. Am. Chem. Soc.* **2014**, *136*, 6479−6488.
(30) Hanna, T. E.; Keresztes, I.; Lobkovsky, E.; Bernskoetter, W. H.; Chirik, P. J. Synthesis of a base-free titanium imido and a transient alkylidene from a titanocene dinitrogen complex. Studies on Ti═NR hydrogenation, nitrene group transfer, and comparison of 1,2-addition rates. *Organometallics* **2004**, *23*, 3448−3458.
(31) Polse, J. L.; Kaplan, A. W.; Andersen, R. A.; Bergman, R. G. Synthesis of an eta(2)-N-2-titanium diazoalkane complex with both imido- and metal carbene-like reactivity patterns. *J. Am. Chem. Soc.* **1998**, *120*, 6316−6328.
(32) (a) Davies, H. M. L.; Antoulinakis, E. G. Intermolecular Metal-Catalyzed Carbenoid Cyclopropanations. In *Organic Reactions*; Overman, L. E., Ed.; John Wiley & Sons: New York, 2001. (b) Davies, H. M. L.; Beckwith, R. E. J. Catalytic enantioselective C-H activation by means of metal-carbenoid-induced C-H insertion. *Chem. Rev.* **2003**, *103*, 2861−2903.
(33) Beckhaus, R.; Santamaria, C. Carbene complexes of titanium group metals - formation and reactivity. *J. Organomet. Chem.* **2001**, *617−618*, 81−97.
(34) Dartiguenave, M.; Menu, M. J.; Deydier, E.; Dartiguenave, Y.; Siebald, H. Crystal and molecular structures of transition metal complexes with N- and C-bonded diazoalkane ligands. *Coord. Chem. Rev.* **1998**, *178-180*, 623−663.
(35) Reich, H. J.; Borst, J. P.; Dykstra, R. R.; Green, D. P. A Nuclear Magnetic Resonance Spectroscopic Technique for the Characterization of Lithium Ion-pair Structures in THF and THF/HMPA Solution. *J. Am. Chem. Soc.* **1993**, *115*, 8728−8741.
(36) Fraenkel, G.; Subramanian, S.; Chow, A. The Carbon-lithium Bond in Monomeric Aryllithiums - Dynamics of Exchange, Relaxation, and Rotation. *J. Am. Chem. Soc.* **1995**, *117*, 6300−6307.
(37) Wu, D.; Chen, A.; Johnson, C. An Improved Diffusion-ordered Spectroscopy Experiment Incorporating Bipolar-Gradient Pulses. *J. Magn. Reson., Ser. A* **1995**, *115*, 260−264.
(38) Jerschow, A.; Muller, N. Suppression of convection artifacts in stimulated-echo diffusion experiments. Double-stimulated-echo experiments. *J. Magn. Reson.* **1997**, *125*, 372−375.
(39) Allen, F. H.; Kennard, O.; Watson, D. G.; Brammer, L.; Orpen, A. G.; Taylor, R. Tables of Bond Lengths Determined by X-ray and Neutron Diffraction. 1. Bond Lengths in Organic Compounds. *J. Chem. Soc., Perkin Trans. 2* **1987**, S1−S19.
(40) Pauling, L. Atomic Radii and Interatomic Distances in Metals. *J. Am. Chem. Soc.* **1947**, *69*, 542−553.
(41) (a) Hazari, N.; Mountford, P. Reactions and applications of titanium imido complexes. *Acc. Chem. Res.* **2005**, *38*, 839−849. (b) Schwarz, A. D.; Nielson, A. J.; Kaltsoyannis, N.; Mountford, P. The first group 4 metal bis(imido) and tris(imido) complexes. *Chem. Sci.* **2012**, *3*, 819−824.
(42) (a) McDade, C.; Green, J. C.; Bercaw, J. E. A Kinetic and Mechanistic Study of the Thermolysis of Bis-(pentamethylcyclopentadienyl)dimethyltitanium(IV). *Organometallics*

DOI: 10.1021/acs.organomet.8b00188
Organometallics XXXX, XXX, XXX−XXX

1982, *1*, 1629−1634. (b) Bulls, A. R.; Schaefer, W. P.; Serfas, M.; Bercaw, J. E. Intramolecular C-H Bond Activation of Benzyl Ligands by Metalated Cyclopentadienyl Derivatives of Permethylhafnocene - Molecular Structure of $(\eta^5\text{-}C_5Me_5)(\eta^5,\eta^1\text{-}C_5Me_4CH_2)HfCH_2C_6H_5$ and the Mechanism of Rearrangement to its Hafnabenzocyclobutene Tautomer $(\eta^5\text{-}C_5Me_5)_2HfCH_2\text{-}o\text{-}C_6H_4$. *Organometallics* **1987**, *6*, 1219−1226.

(43) (a) van Doorn, J. A.; van der Heijden, H.; Orpen, A. G. Tantalum and Titanium Alkylidene Complexes Bearing Phosphinoalkoxide Ligands - Reversible Ortho-metalation of a Titanium Alkylidene. *Organometallics* **1994**, *13*, 4271−4277. (b) van Doorn, J. A.; van der Heijden, H.; Orpen, A. G. Titanium Alkylidenes via Dineopentyl Complexes. *Organometallics* **1995**, *14*, 1278−1283.

(44) (a) Chamberlain, L. R.; Rothwell, I. P.; Huffman, J. C. Intramolecular Activation of Aliphatic Carbon Hydrogen Bonds at Tantalum(V) Metal Centers - A Comparison of Activation by Methyl and Methylidene Functional Groups. *J. Am. Chem. Soc.* **1986**, *108*, 1502−1509. (b) Vilardo, J. S.; Lockwood, M. A.; Hanson, L. G.; Clark, J. R.; Parkin, B. C.; Fanwick, P. E.; Rothwell, I. P. Intramolecular activation of aromatic C-H bonds at tantalum(v) metal centers: evaluating cyclometallation 'resistant' and 'immune' aryloxide ligation. *J. Chem. Soc., Dalton Trans.* **1997**, 3353−3362.

(45) Plundrich, G. T.; Wadepohl, H.; Gade, L. H. Synthesis and Reactivity of Group 4 Metal Benzyl Complexes Supported by Carbazolide-Based PNP Pincer Ligands. *Inorg. Chem.* **2016**, *55*, 353−365.

(46) (a) van der Heijden, H.; Hessen, B. Intermolecular C-H Activation by Reactive Titanocene Alkylidene Intermediates. *J. Chem. Soc., Chem. Commun.* **1995**, 145−146. (b) van der Heijden, H.; Hessen, B. 'Tucked-in' titanocene alkyls and alkylidenes. *Inorg. Chim. Acta* **2003**, *345*, 27−36. (c) Deckers, P. J. W.; Hessen, B. C-H bond activation processes in cationic and neutral titanium benzyl compounds with cyclopentadienyl-arene ligands. *Organometallics* **2002**, *21*, 5564−5575.

(47) Zhang, S.; Tamm, M.; Nomura, K. 1,2-C-H Activation of Benzene Promoted by (Arylimido)vanadium(V)-Alkylidene Complexes: Isolation of the Alkylidene, Benzyne Complexes. *Organometallics* **2011**, *30*, 2712−2720.

(48) Andino, J. G.; Kilgore, U. J.; Pink, M.; Ozarowski, A.; Krzystek, J.; Telser, J.; Baik, M.-H.; Mindiola, D. J. Intermolecular C-H bond activation of benzene and pyridines by a vanadium(III) alkylidene including a stepwise conversion of benzene to a vanadium-benzyne complex. *Chem. Sci.* **2010**, *1*, 351−356.

(49) (a) Wada, K.; Pamplin, C. B.; Legzdins, P.; Patrick, B. O.; Tsyba, I.; Bau, R. Intermolecular activation of hydrocarbon C-H bonds under ambient conditions by 16-electron neopentylidene and benzyne complexes of molybdenum. *J. Am. Chem. Soc.* **2003**, *125*, 7035−7048. (b) Adams, C. S.; Legzdins, P.; Tran, E. C-H activation of substituted arenes by tungsten alkylidene complexes: Products, selectivity, and mechanism. *Organometallics* **2002**, *21*, 1474−1486. (c) Pamplin, C. B.; Legzdins, P. Thermal activation of hydrocarbon C-H bonds by Cp*M(NO) complexes of molybdenum and tungsten. *Acc. Chem. Res.* **2003**, *36*, 223−233.

(50) Cheon, J.; Rogers, D. M.; Girolami, G. S. Mechanistic studies of the thermolysis of tetraneopentyltitanium(IV) 0.1. Solution evidence that titanium alkylidenes activate saturated hydrocarbons. *J. Am. Chem. Soc.* **1997**, *119*, 6804−6813.

(51) Cavaliere, V. N.; Mindiola, D. J. Methane: a new frontier in organometallic chemistry. *Chem. Sci.* **2012**, *3*, 3356−3365.

(52) (a) Bailey, B. C.; Fan, H.; Huffman, J. C.; Baik, M.-H.; Mindiola, D. J. Intermolecular C-H bond activation reactions promoted by transient titanium alkylidynes. Synthesis, reactivity, kinetic, and theoretical studies of the Ti C linkage. *J. Am. Chem. Soc.* **2007**, *129*, 8781−8793. (b) Bailey, B. C.; Fan, H.; Baum, E. W.; Huffman, J. C.; Baik, M.-H.; Mindiola, D. J. Intermolecular C-H bond activation promoted by a titanium alkylidyne. *J. Am. Chem. Soc.* **2005**, *127*, 16016−16017.

(53) (a) Crestani, M. G.; Hickey, A. K.; Gao, X. F.; PInter, B.; Cavaliere, V. N.; Ito, J.-I.; Chen, C. H.; Mindiola, D. J. Room Temperature Dehydrogenation of Ethane, Propane, Linear Alkanes C4-C8, and Some Cyclic Alkanes by Titanium-Carbon Multiple Bonds. *J. Am. Chem. Soc.* **2013**, *135*, 14754−14767. (b) Cavaliere, V. N.; Crestani, M. G.; Pinter, B.; Pink, M.; Chen, C.-H.; Baik, M.-H.; Mindiola, D. J. Room Temperature Dehydrogenation of Ethane to Ethylene. *J. Am. Chem. Soc.* **2011**, *133*, 10700−10703.

(54) Flores, J. A.; Cavaliere, V. N.; Buck, D.; Pinter, B.; Chen, G.; Crestani, M. G.; Baik, M.-H.; Mindiola, D. J. Methane activation and exchange by titanium-carbon multiple bonds. *Chem. Sci.* **2011**, *2*, 1457−1462.

(55) (a) Fan, H.; Fout, A. R.; Bailey, B. C.; Pink, M.; Baik, M.-H.; Mindiola, D. J. Understanding intermolecular C-F bond activation by a transient titanium neopentylidyne: experimental and theoretical studies on the competition between 1,2-CF bond addition and [2 + 2]-cycloaddition/beta-fluoride elimination. *Dalton Trans.* **2013**, *42*, 4163−4174. (b) Kurogi, T.; Carroll, P. J.; Mindiola, D. J. A radical coupled pathway to a stable and terminally bound titanium methylidene. *Chem. Commun.* **2017**, *53*, 3412−3414.

(56) Lindley, B. M.; Swidan, A.; Lobkovsky, E. B.; Wolczanski, P. T.; Adelhardt, M.; Sutter, J.; Meyer, K. Fe(IV) alkylidenes via protonation of Fe(II) vinyl chelates and a comparative Mössbauer spectroscopic study. *Chem. Sci.* **2015**, *6*, 4730−4736.

(57) (a) Franceschi, F.; Solari, E.; Scopelliti, R.; Floriani, C. Metal-mediated transfer of electrons between two different C-C single bonds that function as electron-donor and electron-acceptor units. *Angew. Chem., Int. Ed.* **2000**, *39*, 1685−1687. (b) Crescenzi, R.; Solari, E.; Floriani, C.; Chiesi-Villa, A.; Rizzoli, C. One- and two-electron oxidative pathways leading to cyclopropane-containing oxidized porphyrinogens and C-C-coupled porphyrinogens from alkali cation and transition metal meso-octaethylporphyrinogen complexes. *J. Am. Chem. Soc.* **1999**, *121*, 1695−1706. (c) Gallo, E.; Solari, E.; Re, N.; Floriani, C.; Chiesi-Villa, A.; Rizzoli, C. Carbon-carbon bonds functioning as electron shuttles: The generation of electron-rich manganese(II) Schiff base complexes and their redox chemistry. *J. Am. Chem. Soc.* **1997**, *119*, 5144−5154. (d) Gambarotta, S.; Floriani, C.; Chiesi-Villa, A.; Guastini, C. Carbon-carbon Bond Formation and Cleavage Resulting from a Long-range Metal-promoted Redox Process in the Reactions of Nickel(II) Complexes of N,N′-*ortho*-Phenylenebid(salicylideneamine). *J. Chem. Soc., Chem. Commun.* **1982**, *0*, 756−758. (e) Gambarotta, S.; Mazzanti, M.; Floriani, C.; Zehnder, M. A Tetranuclear Polyfunctional Sodium-vanadium(III) Complex Containing a Vanadium(III)-vanadium(III) Double-bond. *J. Chem. Soc., Chem. Commun.* **1984**, *0*, 1116−1118. (f) Gambarotta, S.; Urso, F.; Floriani, C.; Chiesivilla, A.; Guastini, C. Carbon-carbon Bond Forming and Breaking by a Metal-assisted Redo Process in a Nickel(II) Schiff-base Complex. *Inorg. Chem.* **1983**, *22*, 3966−3972.

(58) Hulley, E. B.; Wolczanski, P. T.; Lobkovsky, E. B. Carbon-carbon Bond Formation from Azaallyl and Imine Couplings About Metal-metal Bonds. *J. Am. Chem. Soc.* **2011**, *133*, 18058−18061.

(59) Frazier, B. A.; Williams, V. A.; Wolczanski, P. T.; Bart, S.; Meyer, K.; Cundari, T. R.; Lobkovsky, E. B. C-C Bond Formation and Related Reactions at the CNC Backbone in (smif)FeX (smif = 1,3-di-(2-pyridyl)-2-azaallyl): Dimerizations, 3 + 2 Cyclization, and Nucleophilic Attack; Transfer Hydrogenations and Alkyne Trimerization (X = $N(TMS)_2$, dpma (di-(2-pyridyl-methyl)-amide)). *Inorg. Chem.* **2013**, *52*, 3295−3312.

(60) Williams, V. A.; Hulley, E. B.; Wolczanski, P. T.; Lancaster, K. M.; Lobkovsky, E. B. Pushing the limits of redox non-innocence: pseudo square planar $[\{\kappa^4\text{-}Me_2C(CH_2N{=}CHpy)_2\}Ni]^n$ (n = 2+, 1+, 0, −1, −2) favor Ni(II). *Chem. Sci.* **2013**, *4*, 3636−3648.

(61) Williams, V. A.; Wolczanski, P. T.; Sutter, J.; Meyer, K.; Cundari, T. R.; Lobkovsky, E. B. Iron Complexes Derived from $\{nacnac\text{-}(CH_2py)_2\}^-$ and $\{nacnac\text{-}(CH_2py)(CHpy)\}^n$ Ligands: Stabilization of Fe(II) via Redox Non-innocence. *Inorg. Chem.* **2014**, *53*, 4459−4474.

(62) Morris, W. D.; Wolczanski, P. T.; Sutter, J.; Meyer, K.; Cundari, T. R.; Lobkovsky, E. B. Iron and Chromium Complexes Containing Tridentate Chelates Based on Nacnac and Imino- and Methyl-

DOI: 10.1021/acs.organomet.8b00188
Organometallics XXXX, XXX, XXX−XXX

Pyridine Components: Triggering C-C(X) Bond Formation. *Inorg. Chem.* **2014**, *53*, 7467−7484.
(63) Hulley, E. B.; Williams, V. A.; Morris, W. D.; Wolczanski, P. T.; Hernández-Burgos, K.; Lobkovsky, E. B.; Cundari, T. R. Disparate Reactivity from Isomeric $\{Me_2C(CH_2N{=}CHpy)_2\}$ and $\{Me_2C(CH{=}NCH_2py)_2\}$ Chelates in Iron Complexation. *Polyhedron* **2014**, *84*, 182−191.
(64) Lindley, B. M.; Wolczanski, P. T.; Cundari, T. R.; Lobkovsky, E. B. 1st Row Transition Metal and Lithium Pyridine-ene-amide Complexes Exhibiting N- and C-Isomers and Ligand-based Activation of Benzylic C-H Bonds. *Organometallics* **2015**, *34*, 4656−4688.
(65) Jacobs, B. P.; Wolczanski, P. T.; Lobkovsky, E. B. Oxidatively Triggered Carbon-carbon Bond Formation in Ene-amide Complexes. *Inorg. Chem.* **2016**, *55*, 4223−4232.
(66) (a) Dzik, W. I.; Xu, X.; Zhang, X. P.; Reek, J. N. H.; de Bruin, B. 'Carbene Radicals' in Co-II(por)-Catalyzed Olefin Cyclopropanation. *J. Am. Chem. Soc.* **2010**, *132*, 10891−10902. (b) Dzik, W. I.; Zhang, X. P.; de Bruin, B. Redox Noninnocence of Carbene Ligands: Carbene Radicals in (Catalytic) C-C Bond Formation. *Inorg. Chem.* **2011**, *50*, 9896−9903.
(67) Dzik, W. I.; de Bruin, B. Open-shell organometallics: reactivity at the ligand. *Organometallic Chemistry* **2011**, *37*, 46.
(68) Branchadell, V.; Muray, E.; Oliva, A.; Ortuño, R. M.; Rodríguez-García, C. Theoretical study of the mechanism of the addition of diazomethane to ethylene and formaldehyde. Comparison of conventional ab initio and density functional methods. *J. Phys. Chem. A* **1998**, *102*, 10106−10112.
(69) Kornecki, K. P.; Briones, J. F.; Boyarskikh, V.; Fullilove, F.; Autschbach, J.; Schrote, K. E.; Lancaster, K. M.; Davies, H. M. L.; Berry, J. F. Direct Spectroscopic Characterization of a Transitory Dirhodium Donor-Acceptor Carbene Complex. *Science* **2013**, *342*, 351−354.
(70) Solowey, D. P.; Mane, M. V.; Kurogi, T.; Carroll, P. J.; Manor, B. C.; Baik, M.-H.; Mindiola, D. J. A new and selective cycle for dehydrogenation of linear and cyclic alkanes under mild conditions using a base metal. *Nat. Chem.* **2017**, *9*, 1126−1132.

DOI: 10.1021/acs.organomet.8b00188
Organometallics XXXX, XXX, XXX−XXX